

Subsidence Monitoring at Lost Hills Oil Field with SAR Interferometry and Other Remote Technologies

a project under

SOLID EARTH AND NATURAL HAZARDS RESEARCH AND APPLICATIONS

NRA-01-OES-05

**Final report
October 2005**

Eric Fielding, PI
Ronald Blom, Co-I
Earth Science Section 3242

Jet Propulsion Laboratory
California Institute of Technology
Pasadena, California 91109

Table of Contents

Subsidence Monitoring at Lost Hills Oil Field with SAR Interferometry and Other Remote Technologies.....	1
Background	3
Data Used	3
Measurement errors	7
Processing issues	11
Recommendations for future studies	18
Application technology benefits	18
References.....	18

Background

This project is an extension and continuation of synthetic aperture radar (SAR) interferometry studies of Lost Hills oil field with data from the identical radar systems on the two European Remote Sensing (ERS) satellites (Brink et al., 2002; Fielding et al., 1998; Patzek et al., 2001). The ERS-1 satellite operated from 1991 to early 2000. The ERS-2 satellite served from 1995 to January 2001 with full performance and continues to the present with partial operation. The ERS-2 satellite has been working since January 2001 without gyroscopes to control its orientation, so many images are not usable for interferometry. The Radarsat-1 satellite was launched in November 1995 and continues to operate as of the writing of this report. The details of the SAR interferometry technique are not described in this brief report. See Bürgmann, Rosen and Fielding (Bürgmann et al., 2000) and Rosen et al. (Rosen et al., 2000) for more details on InSAR.

Data Used

In this project, interferometric analysis of Radarsat-1 SAR data was used to measure subsidence rates over the Lost Hills, California oil field during the fall of 2002 and early 2003. The Radarsat-1 satellite has several SAR operation modes, with different spatial resolutions and different incidence angles. It also acquires data on ascending orbits where the satellite is moving northward and SAR looking roughly east, and on descending orbits where the satellite is moving southward and SAR looking roughly west. The Radarsat-1 data used in this report were acquired in four different modes and both ascending and descending orbits. Note that only SAR data acquired in the same beam mode can be combined into interferograms so data from different beams forms disjoint datasets.

The Radarsat-1 satellite repeats the same track every 24 days so that there is the potential for interferometric pairs with intervals that are multiples of 24 days. Interferometric pairs of Radarsat-1 scenes obviously require that the satellite be in operation and image the Lost Hills area on the two dates at the beginning and end of the interval. Fortunately, a large number of Radarsat-1 images have been acquired since the beginning of 2002 for the area of the western San Joaquin Valley that includes Lost Hills. A subset of 14 of the acquired scenes was selected for analysis in this project (See Table 1). An additional requirement is that the two satellite orbits must be close enough to each other, within a few hundred meters, as described next.

image ID	date	orbit	beam mode
1	8/31/02	35615	F1d
2	9/24/02	35958	F1d
3	10/18/02	36301	F1d
4	11/11/02	36644	F1d
5	4/4/03	38702	F1d
6	10/14/02	36237	F2a
7	11/7/02	36580	F2a
8	1/18/03	37609	F2a
9	9/3/02	35658	S1d
10	10/21/02	36344	S1d
11	9/10/02	35751	S2a
12	10/4/02	36094	S2a
13	10/28/02	36437	S2a
14	1/8/03	37466	S2a

Table 1. List of Radarsat-1 scenes selected for analysis.

The distance between the satellite orbits for an interferometric pair is called the spatial baseline. A list of the interferogram pairs that have been processed appears in Table 2. The absolute position of the orbits is not important, only the baseline between them (see last column in Table 2). Figure 1 shows a plot of the positions of the orbits for the descending Radarsat-1 track that images Lost Hills with Fine Beam F1 against the acquisition date. In fact, only the component of the baseline that is perpendicular to the radar look direction (line from the satellite to the ground) affects the quality of the interferogram, so the plot in Figure 1 and the baseline column of Table 2 only show only the perpendicular component of the position. The vertical axis distance between any two scenes plotted on Figure 1 is the perpendicular baseline. The five Radarsat-1 scenes that were selected from beam mode F1, descending, are marked in Figure 1 with their dates of acquisition in larger red numbers. The smaller numbers are the Radarsat-1 orbit numbers.

Interfero-gram ID	start date	end date	beam mode	Orbit direction	length (days)	baseline (m)
1	8/31/02	9/24/02	F1d	D	24	90
2	9/24/02	10/18/02	F1d	D	24	120
3	10/18/02	11/11/02	F1d	D	24	50
4	9/10/02	10/4/02	S2a	A	24	55
5	10/4/02	10/28/02	S2a	A	24	110
6	10/14/02	11/7/02	F2a	A	24	110
7	9/3/02	10/21/02	S1d	D	48	25
8	9/10/02	10/28/02	S2a	A	48	110
9	8/31/02	10/18/02	F1d	D	48	30
10	9/24/02	11/11/02	F1d	D	48	170
11	8/31/02	11/11/02	F1d	D	72	80
12	11/7/02	1/18/03	F2a	A	72	110
13	10/4/02	1/8/03	S2a	A	96	115
14	11/11/02	4/4/03	F1d	D	144	350
15	9/24/02	4/4/03	F1d	D	192	180

Table 2. List of Radarsat-1 interferograms processed, in order of increasing time interval length.

The longer the baseline, the worse the coherence of the interferogram due to spatial decorrelation of the SAR (Fielding et al., 2005; Rosen et al., 2000; Zebker and Villasenor, 1992). The coherence degrades gradually so there is not a sharp cut-off for baseline, but increasing coherence or decorrelation results in additional noise in the interferogram. To form a good quality interferogram, the baseline should be less than about 600 meters for the Radarsat-1 Fine Beams and less than about 300 meters for the Radarsat-1 Standard Beams (and also for the ERS satellites). The Canadian Space Agency has been maintaining the orbit of the Radarsat-1 satellite within a band about 2000 meters wide since late 2001 (before then they used a 5000 meter band). This means that a good number of the orbits form pairs with baselines suitable for interferometry, but not every pair is suitable.

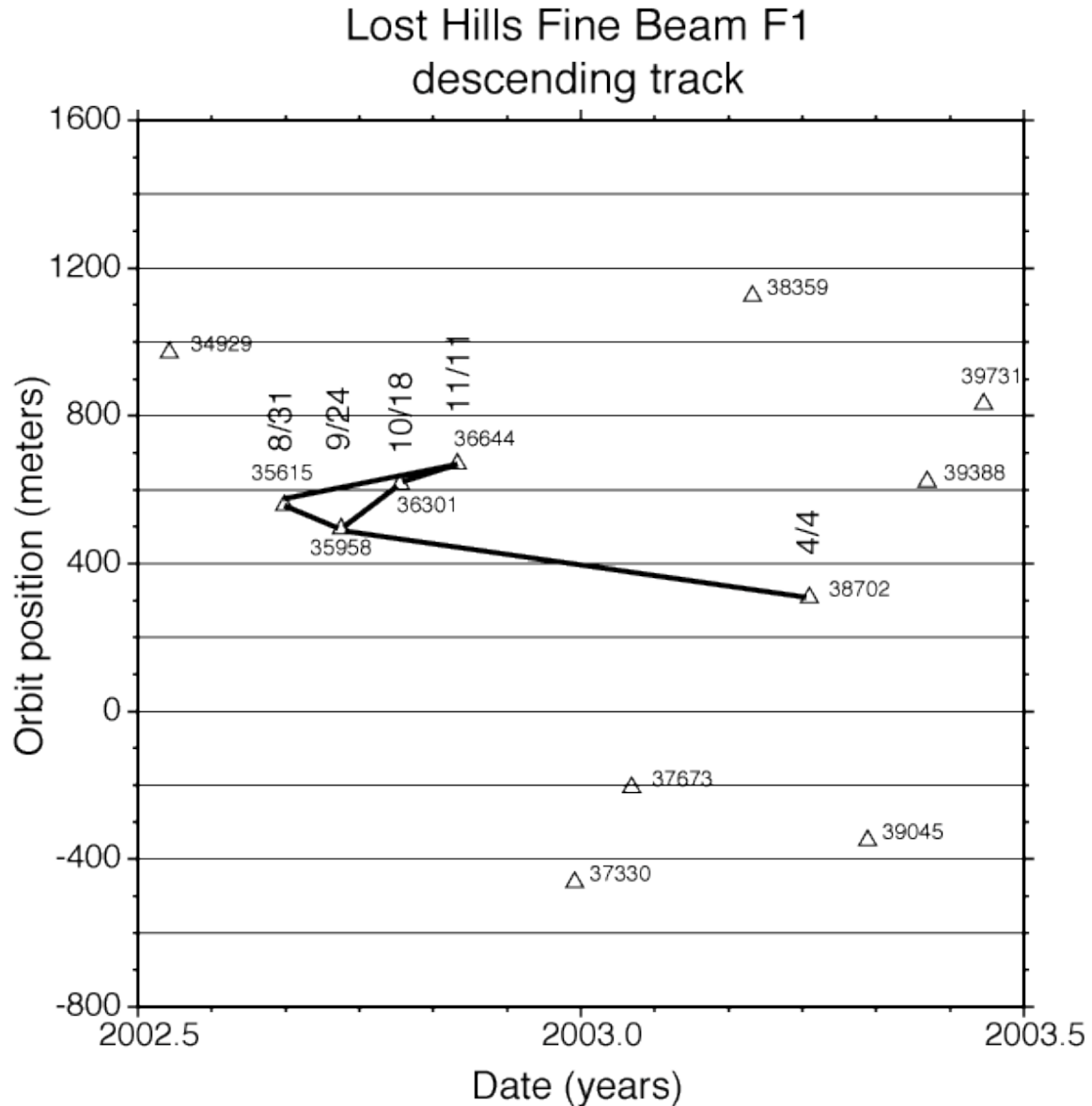


Figure 1. Plot of Radarsat-1 satellite orbit position (perpendicular to SAR look direction) versus acquisition time. Triangles mark scenes that imaged the Lost Hills area in Fine Beam F1 between July 2002 and June 2003 (inclusive). Thick black lines link pairs of scenes used to form interferograms. Small numbers are orbit numbers and larger numbers show the dates of the interferogram scenes.

The four Radarsat-1 orbits that imaged Lost Hills with Beam F1 on 8/31/02, 9/24/02, 10/18/02, and 11/11/02 all happened to be close together (Figure 1). This means that interferograms can be formed from any two of these four orbits. The orbit on 4/4/03 was close enough to the 9/24/02 orbit to have a roughly 190 meter baseline which is long enough to cause some decorrelation in the interferogram. The baseline between the 4/4/03 orbit and the 11/11/02 orbit is almost 400 meters,

which could cause a substantial degradation of the interferogram. Unfortunately, the other Radarsat-1 acquisitions between November 2002 and April 2003 are much farther away from the other scenes investigated here (Figure 1). The December 2002 and January 2003 scenes should form a 24-day pair between themselves (not evaluated). An interferogram between the November and December 2002 Radarsat-1 F1 scenes would have a baseline of about 1000 meters and likely poor coherence due to spatial decorrelation. Because of the flat topography in the immediate area of the oil fields, however, a special InSAR processing technique called “spectral shift filtering” can largely mitigate the effects of spatial decorrelation (e.g., Fielding et al., 2005). In areas of steeper slopes, this special filtering technique is not effective.

Measurement errors

SAR interferometry has two major types of error that are relevant for measuring subsidence over a small area such as an oil field. One type of error is “white” noise (random over very short distances) due to decorrelation, and the other type is medium-wavelength error due to variations in atmospheric conditions. The decorrelation tends to increase with time (as described below) but the atmospheric errors are more independent of time, so the longer time intervals are less affected by atmospheric errors relative to the subsidence signal. The second dimension plotted in Figure 1 is time, so the time interval for each pair of scenes is shown by the distance between them on the horizontal axis. The length of the time interval has several important effects on the interferometric measurements of subsidence. If the subsidence rate is constant with time then the surface elevation change obviously increases linearly with the time interval, so the longer the interval the larger the observable signal unless decorrelation becomes severe.

Decorrelation is one of the important sources of error in interferometric measurements (Fielding et al., 2005). In addition to the spatial-baseline decorrelation described above, there is also temporal decorrelation of the interferogram due to changes in the ground surface between the two SAR images. In most areas, these changes increase with time (trees and bushes grow, farm fields get plowed, oil field equipment gets moved, rain washes away some of the soil, etc.) so the coherence of the interferograms degrades with time. The SAR interferometry process measures the one phase change value for the radar return from a patch of ground surface with an area that depends on the SAR mode. This phase value is proportional to the surface elevation change. For Radarsat-1 Standard Beams, the fundamental surface patch is roughly 20 x 5 meters, while Radarsat-1 Fine Beams patches are about 10 x 5 meters. The more disruption to the ground and objects in a patch, the more decorrelation of the interferometric measurement for that patch. Complete disruption, such as plowing, destroys the interferometric

information for that patch and returns a random phase value. The SAR processing always includes some spatial averaging or smoothing over adjacent ground patches, so the measured values in the final products depend on areas that are much greater than the fundamental SAR resolution, usually 40 x 40 meters or 80 x 80 meters. This greatly reduces the noise from any one patch because the decorrelation noise is random from one patch to the next.

The second important source of error in SAR interferograms is atmospheric changes. Variations in the atmosphere, primarily water vapor content that is sometimes but not always associated with clouds, above the ground affect the radar propagation and the measured phase. Because an interferogram differences two radar images, it is the difference between the atmospheric conditions at the times of the two radar acquisitions that affects the interferometric measurements. Water vapor variations have a magnitude that increases with increasing spatial scale (typically a power law distribution) up to a spatial scale of 5–10 km (Goldstein, 1995). One way to see the effects of these atmospheric changes is to compare independent interferograms covering the same time interval. Because the Radarsat-1 satellite has multiple beam modes, it can image the same location several times during its repeat cycle. Interferograms from different beams will have scenes acquired at different times, usually a few days apart.

Early September to mid-October 2002 48-day Radarsat-1 interferograms

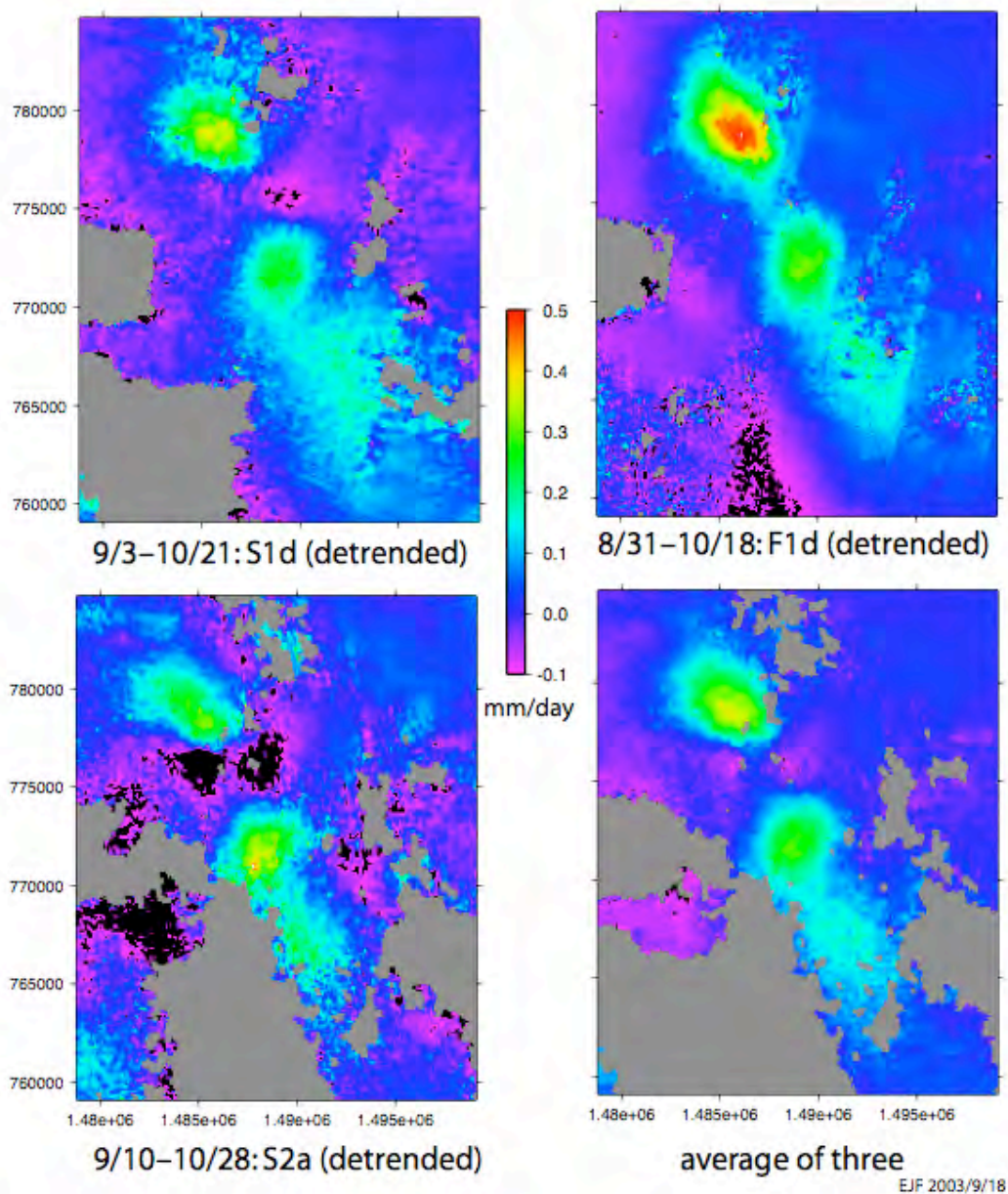


Figure 2. Comparison of three interferograms (IDs 7, 9, and 8 in Table 2) for overlapping time intervals in September and October 2002 and the average of the three interferograms.

Figure 2 shows three interferograms for the period between early September and mid-October 2002. These were acquired in beam modes

S1 and F1 on descending orbits and S2 on ascending orbits. Each interferogram was converted to vertical motion assuming no horizontal motion, which is a first-order correction for the different incidence angles of the different beams. In addition, the three interferograms had a trend removed (see more discussion below). The fourth panel shows the average of the three interferograms. Since the 48-day time intervals of the three interferograms overlap almost completely (except for ten days on both ends), the variations between the interferograms must be due primarily to atmospheric changes. This is an important caution for interpreting a single interferogram, even with a longer 48-day interval. The average interferogram is a much more accurate measure of the subsidence pattern during that time. This kind of averaging or "stacking" of interferograms is a simple way of combining interferograms. Other techniques have recently been developed to more effectively combine a series of interferograms into a deformation time history and use the redundancy to reduce the atmospheric effects (Berardino et al., 2002; Schmidt and Bürgmann, 2003; Usai, 2003). This subject is recommended for more study and application to the Lost Hills subsidence. Blue tones are approximately zero motion and magenta-purple tones are apparent uplift.

Figure 3 shows a similar average interferogram in panel (f), but with an average of five interferograms, including the three used in Figure 2 plus two more with later time intervals extending as late as January 2003. Again, all interferograms have been converted to vertical motion with the assumption of no horizontal motion, and they have been detrended. Four of the interferograms have 48-day intervals and one has a 96-day interval. These figures show the entire area used in the detrending procedure. This figure also shows a much larger area around Lost Hills to give a more regional view. The first five panels (Figure 3a-e) show difference images calculated by subtracting each individual interferogram from the average of the five. If we assume that the subsidence rate at Lost Hills remained constant over the time interval between the end of August 2002 and early January 2003 and the average is a good approximation of the subsidence pattern, then these difference images show the errors in each of the interferograms.

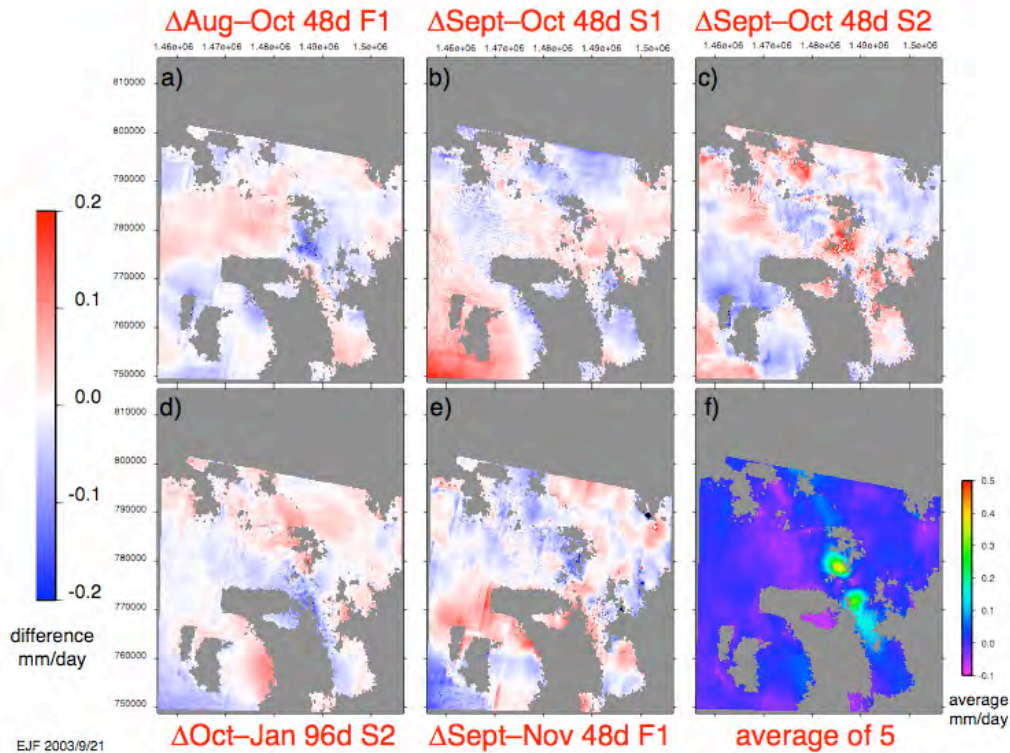


Figure 3. Difference images for five interferograms (a-e; IDs 9, 7, 8, 13, and 10, respectively in Table 2) with blue-red color scale shown at left. Average of the five interferograms is shown in panel (f) with the color scale at right. Difference images are the average minus each individual interferogram.

The “cloudy” shapes to the positive and negative anomalies or errors in the difference images of Figure 3 are consistent with the InSAR errors being due to variations in the atmospheric water vapor content. The magnitude of the errors in these individual interferograms are about 5–10 mm of range change before dividing by the time interval. This is consistent with the atmospheric errors found by other studies (Goldstein, 1995; Wright et al., (in preparation); Zebker et al., 1997). After converting the interferograms to rates, dividing by the time interval, the rate errors vary with some interferograms shown in Figure 3 having +/- 0.2 mm/day errors and others having errors less than +/- 0.1 mm/day. Because these atmospheric errors are independent of the interferogram interval, interferograms with shorter time intervals, such as the minimum of 24 days possible with Radarsat-1, will have greater errors in the estimate of subsidence rate roughly +/- 0.2 to 0.4 mm/day.

Processing issues

The results presented in this report use a standard local coordinate system called State Plane coordinates. In the area of the Lost Hills oil

field, the local system is California State Plane zone 5 (called CA5 for brevity), which is a specific implementation of a Lambert Conformal Conic projection (standard parallels $34^{\circ} 2' N$ and $35^{\circ} 28' N$, projection origin $118^{\circ} 0' W$, $33^{\circ} 30' N$). The horizontal distance units are feet, and the horizontal datum is NAD27 (North American Datum of 1927). This coordinate system was used for maximum compatibility with ChevronTexaco, the project collaborator. The SAR interferometry data was processed in SAR image coordinates and then rectified to a geographic (equi-angular; equal spacing in latitude and longitude) projection using a digital elevation model from the National Elevation Database with a spacing of 1-arcsecond (roughly 30 meters). The InSAR results were then projected from the geographic projection to the CA5 projection with a grid spacing of 98.425 feet (30 meters).

It is very important to note that the SAR interferometry measurements are "range change" or a measurement of the difference in range between the satellite and the ground. This measurement is made in the direction between the ground and the satellite, so the measured motion is not purely vertical. This means that the interferometric range change sees a mixture of horizontal and vertical motions that depends on the incidence angle or angle that the radar beam hits the ground. The incidence angles, measured from the vertical, are different for each Radarsat-1 beam as shown in Table 3. (The incidence angle also changes somewhat across the radar image, but for a small area the incidence angle is approximately constant.) For example, with Radarsat-1 beam mode F1 on descending orbits, the angle is about 38 degrees away from the vertical (Table 3), in a direction that is roughly east. The main effect of this angle is that the interferometric range change sees only 78% of the vertical subsidence motion (cosine of the incidence angle). (The measured range change is the dot product between the ground-to-satellite vector and the ground motion vector.) The range change is also sensitive to the horizontal motions, which are multiplied by the sine of the incidence angle (see Table 3) and also multiplied by the cosine of the angle between the ground motion vector and the satellite location vector (close to 1.0 for east-west displacements).

beam mode	incidence		
	angle (degrees)	cosine(inc. ang.)	sine(inc. ang.)
S1	23.21	0.919	0.394
S2	27.7	0.885	0.465
F1	38.4	0.784	0.621
F2	40.68	0.758	0.652
F3	42.75	0.734	0.679
F4	44.72	0.711	0.704

Table 3. Radarsat-1 beam mode incidence angles and their cosines and sines.

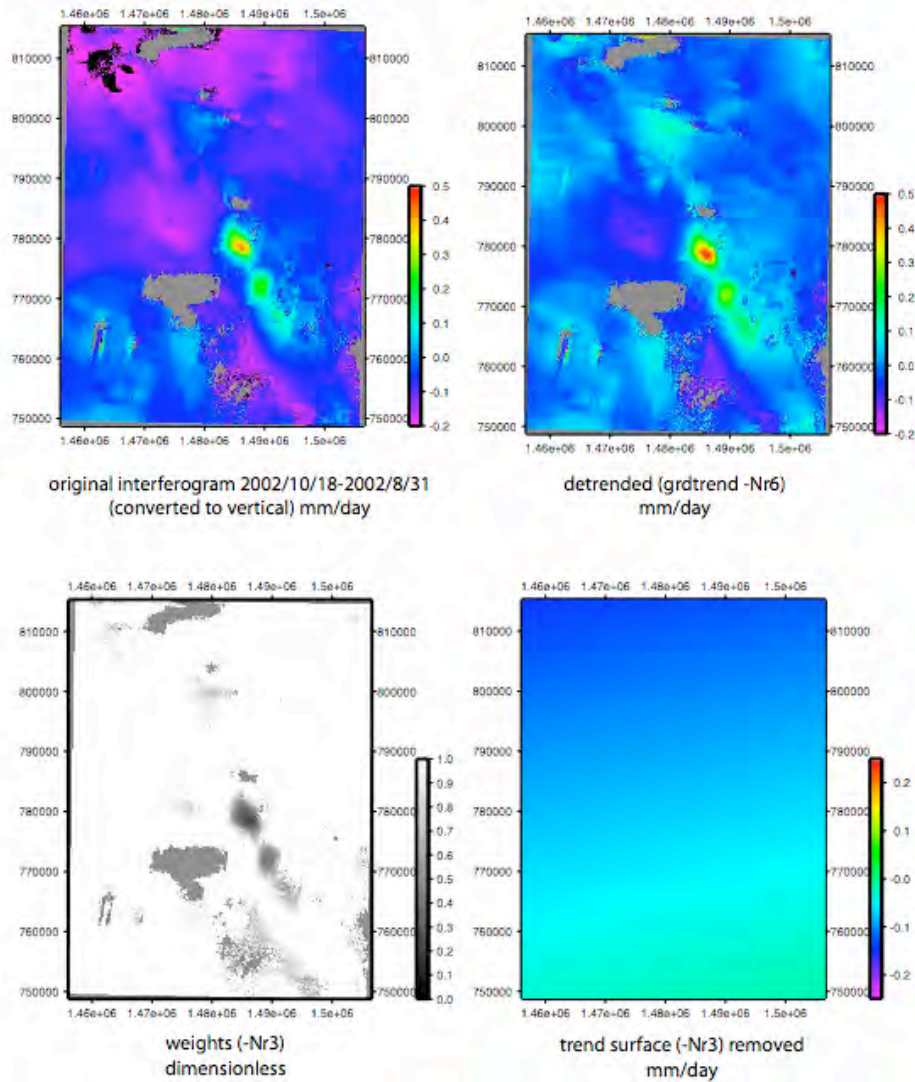
For Radarsat-1 standard beams S1 and S2, the range change is much less sensitive to the horizontal motions than the vertical (Table 3). For the fine beams F1 and F2 investigated in this report, the sensitivity to the vertical is still substantially greater than to the horizontal. Since the Lost Hills reservoir is quite shallow (on the order of 700 meters or 2000 feet), the horizontal motions are generally smaller than the vertical. Because the horizontal motions are smaller than the vertical and the satellite is less sensitive to the horizontal, the horizontal motions are ignored in the first-order analysis presented here. Fine beams F3 and F4 have almost equal sensitivity to horizontal and vertical motion, so it will be more important to consider the horizontal motions when InSAR data from these beams are used. The horizontal component also changes sign, depending on whether the radar data is acquired on ascending orbits with the satellite west of the oil field or on descending orbits where the satellite is to the east. For example with a descending orbit and an oil field that is trending roughly north-south, on the east side of the subsidence bowl the ground surface moves to the west and adds a small additional amount to the range change, while on the west side the ground surface moves east and subtracts from the range change. The horizontal motion has the opposite effect for InSAR data from ascending orbits (see Tables 1 and 2 for the orbit directions of the interferograms).

There is an additional type of error that commonly affects interferograms due to imprecise knowledge of the baseline between the orbits. This type of error, usually called “orbit error”, appears as a linear or quadratic trend across the entire scene. The accuracy of the Radarsat-1 orbit locations is poorer than for the ERS and Envisat satellites, so the orbit errors in Radarsat-1 interferograms tend to be larger. Part of the processing sequence used here takes the observed interferometric phase variation across the scene and calculates an effective baseline for the pair that will mitigate the orbit error. The very longest wavelength variations of the atmospheric water vapor, as described above, can affect the apparent orbit error so the calculated baseline may differ from the true distance between the orbits in space.

The errors due to atmospheric water variations over medium-to-long wavelengths (and any long-wavelength orbit error remaining) can be removed empirically by doing a local fit to the phase variations to measure a trend and then removing it. This process is called “detrending” and was applied to the InSAR measurements in Figures 2 and 3 before the averaging and differencing. The detrending also removes a constant from the data to adjust the zero level of the interferogram. The area surrounding the Lost Hills oil field used for the trend fitting is shown in Figures 3–5. The 48-day beam F1 interferogram with ID 9 (see Table 2) is plotted in Figure 4a after conversion to vertical motion and before detrending. In Figure 4b, the interferogram is plotted after fitting a linear trend surface (with three coefficients: a constant and linear coefficients of X and Y) and removing it. Panel 4c shows the trend surface that was removed.

The program used for detrending, “grdtrend” in the Generic Mapping Tools package (Wessel and Smith, 1991, 1998), has an option for what they call robust trend fitting. This option causes the program to do an iterative process of fitting the data, locating regions of outliers, calculating a weighting map to reduce the weight of the outliers, and then fitting the data again using the weighting. This option was used in the trend fit of Figure 4, and the final weighting map is shown in panel 4d. The robust trend fitting does a good job of automatically lowering the weight of the Lost Hills subsidence signal compared to the surrounding area so that the trend surface fit is not affected by the signal we want to measure.

Lost Hills interferogram trend removal



grdtrend Robust iteration 1: Old Chi Squared: 1074.84 New Chi Squared 401242
 Coefficient fit to Mean: -0.0756703
 Coefficient fit to X: 0.00897827
 Coefficient fit to Y: 0.055706

EJF 2003/9/16

Figure 4. Detrending procedure inputs and outputs using a linear (3-parameter) robust fit.

The detrending can also be done with higher order fits. Figure 5 shows a fit with six parameters to the same data used in Figure 4. The first three parameters are the same as in the three-parameter fit: a constant offset and linear coefficients of X and Y. The second three parameters are

higher order terms: a coefficient of $X*Y$, and coefficients of X^2 and Y^2 . The detrended interferogram in the area of the Lost Hills oil field is not very different between the 3-parameter and 6-parameter fits for this case. Interferograms with a substantial amount of curvature in the phase signal due to atmospheric effects should work better with the higher order fit, but it does not seem to be necessary for this size of area.

Lost Hills interferogram trend removal

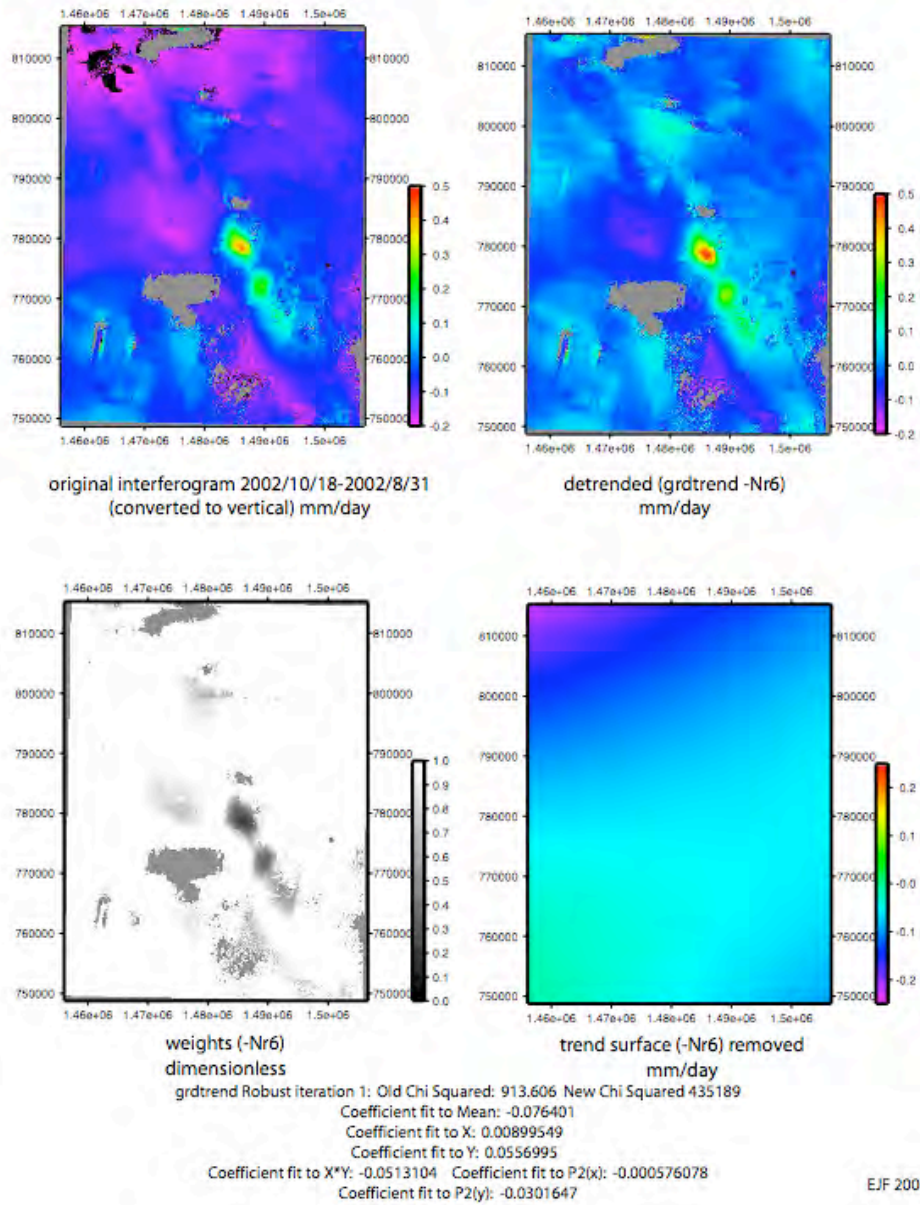


Figure 5. Detrending with robust six-parameter fit, for same input data as Figure 4.

Recommendations for future studies

The fastest subsidence rates at Lost Hills in 2002 were about 0.4 mm/day, so the atmospheric errors in the 24-day interferograms can be 50% to 100% of the signal. A single 24-day interferogram is not an accurate measurement. Interferograms with moderate lengths of 48 to 96 days have reduced effects of the atmospheric errors compared to the ongoing subsidence signal. Longer interferogram intervals, such as the 144- and 192-day interferograms investigated here should have a better signal-to-atmospheric noise ratio, but they suffer from greater decorrelation that makes the InSAR phase difficult to measure and unwrap.

Application technology benefits

The ultimate goal of this project was to develop the InSAR technique for monitoring the Lost Hills oil field and transition to an operational system. This goal was completely fulfilled as the main Lost Hills oil field operator, a subsidiary of ChevronTexaco, is now purchasing regular InSAR products from a commercial remote sensing company (formerly called Atlantis Scientific Inc., then Vexcel Canada and now a part of Microsoft's Virtual Earth business unit since May 2006) and they using the data to optimize their operations of the oil field processes.

References

- Berardino, P., Fornaro, G., Lanari, R., and Sansosti, E., 2002, A new algorithm for surface deformation monitoring based on small baseline differential SAR interferograms: *Geoscience and Remote Sensing, IEEE Transactions on*, v. 40, no. 11, p. 2375-2383.
- Brink, J., Patzek, T.W., Silin, D.B., and Fielding, E.J., 2002, SPE77646: Lost Hills field trial—incorporating new technology for reservoir management, *SPE Annual Technical Conference and Exhibition: San Antonio, Texas*.
- Bürgmann, R., Rosen, P.A., and Fielding, E.J., 2000, Synthetic aperture radar interferometry to measure Earth's surface topography and its deformation: *Annual Review of Earth and Planetary Sciences*, v. 28, p. 169-209.
- Fielding, E.J., Blom, R.G., and Goldstein, R.M., 1998, Rapid subsidence over oil fields measured by SAR interferometry: *Geophys. Res. Lett.*, v. 25, p. 3215–3218.
- Fielding, E.J., Talebian, M., Rosen, P.A., Nazari, H., Jackson, J.A., Ghorashi, M., and Berberian, M., 2005, Surface ruptures and building damage of the 2003 Bam, Iran earthquake mapped by satellite synthetic aperture radar interferometric correlation:

- Journal of Geophysical Research, v. 110, no. B3, p. B03302, doi:10.1029/2004JB003299.
- Goldstein, R., 1995, Atmospheric limitations to repeat-track radar interferometry: Geophysical Research Letters, v. 22, no. 18, p. 2517–2520.
- Patzek, T.W., Silin, D.B., and Fielding, E.J., 2001, SPE71610: Use of satellite radar images in surveillance and control of two giant oilfields in California, SPE Annual Technical Conference and Exhibition, Volume 71610: New Orleans, Louisiana, USA, Society of Petroleum Engineers.
- Rosen, P.A., Hensley, S., Joughin, I.R., Li, F.K., Madsen, S.N., Rodriguez, E., and Goldstein, R.M., 2000, Synthetic aperture radar interferometry: Proceedings of the IEEE, v. 88, no. 3, p. 333-382.
- Schmidt, D.A., and Bürgmann, R., 2003, Time-dependent land uplift and subsidence in the Santa Clara valley, California, from a large interferometric synthetic aperture radar data set: Journal of Geophysical Research, v. 108, no. B9, p. 2416.
- Usai, S., 2003, A least squares database approach for SAR interferometric data: Geoscience and Remote Sensing, IEEE Transactions on, v. 41, no. 4, p. 753-760.
- Wessel, P., and Smith, W.H.F., 1991, Free software helps map and display data: Eos, Transactions, American Geophysical Union, v. 72, p. 441.
- , 1998, New, improved version of the Generic Mapping Tools released: Eos, Transactions, American Geophysical Union, v. 79, p. 579.
- Wright, T.J., Clarke, P.J., and Funning, G.J., (in preparation), Realistic errors for models derived from InSAR: how reliable are earthquake slip distributions: Journal of Geophysical Research.
- Zebker, H.A., Rosen, P.A., and Hensley, S., 1997, Atmospheric effects in interferometric synthetic aperture radar surface deformation and topographic maps: Journal of Geophysical Research, v. 102, no. B4, p. 7547–7563.
- Zebker, H.A., and Villasenor, J., 1992, Decorrelation in interferometric radar echoes: IEEE Transactions on Geoscience and Remote Sensing, v. 30, no. 5, p. 950–959.